

B. Pimpanuwat<sup>\*1</sup>, M. D. Gray<sup>1,2</sup>, S. Etoka<sup>1</sup>, W. Homan<sup>3</sup>, A. M. S. Richards<sup>1</sup> and ATOMIUM consortium

<sup>1</sup>JBCA, the University of Manchester, UK; <sup>2</sup>National Astronomical Research Institute of Thailand, TH; <sup>3</sup>Université Libre de Bruxelles, BE

## Introduction

Fully 3D modelling remains one of the most active topics in theoretical maser research. Older models only consider specific cloud geometries<sup>[1],[2]</sup>.

A 3D modelling code for maser flares at VLBI scale (*maser3D*)<sup>[3],[4],[5]</sup> has been in development for constructing maser models with more realistic physical conditions, including e.g.

- ❖ Truly 3D geometric consideration
- ❖ multi-cloud systems
- ❖ cloud shape and orientation
- ❖ 3D velocity profiles
- ❖ multiple sources of radiation

Comparing the models to observations will shed some light on how masers are generated in the circumstellar envelopes (CSE) of AGB stars.

Here we present the latest upgrades to *maser3D* and its first results of masers towards AGB stars, with special reference to  $\pi^1$  Gru (see also our poster on the ALMA observations of O-rich evolved stars for more context).

## Development of *maser3D*

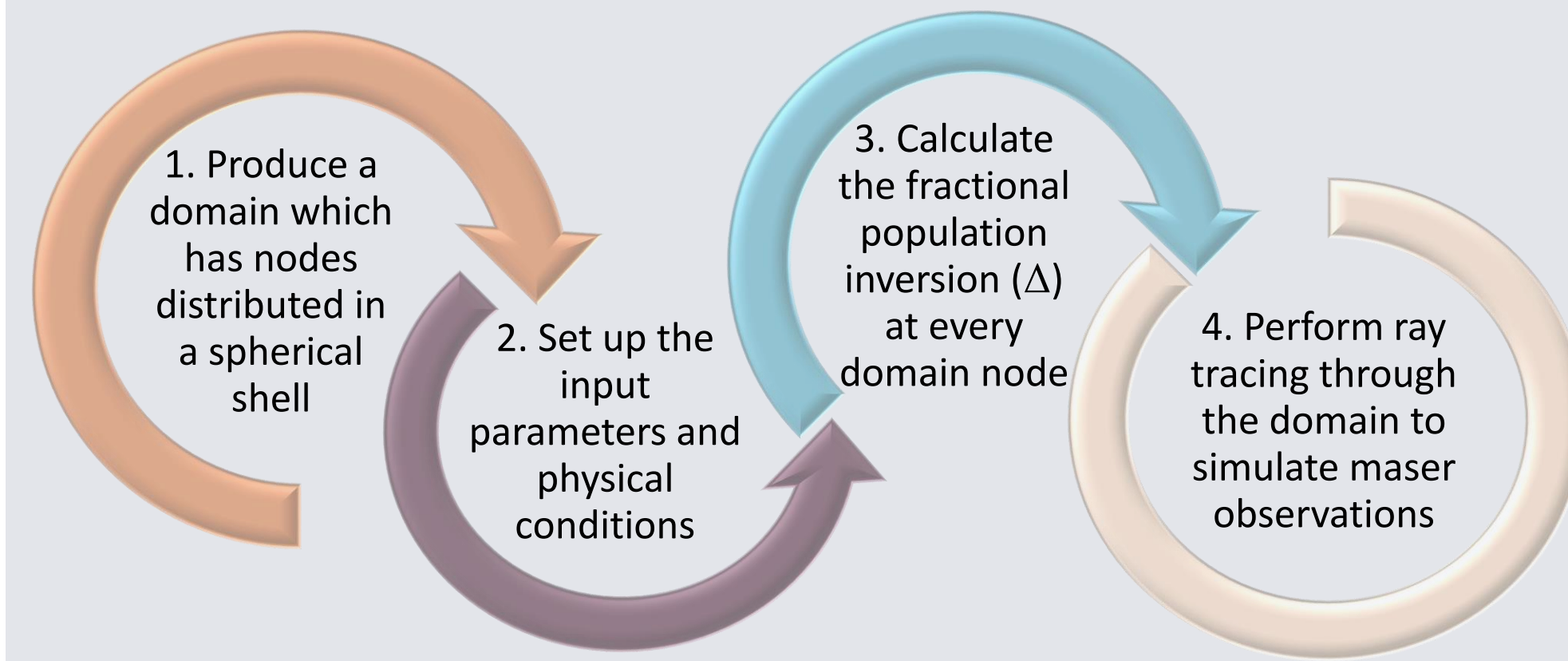


Figure 1. Diagram summarising the steps required to obtain simulated spectra and VLBI images using the *maser3D* code. See [3] for a detailed description.

### New functionalities:

- ❖ Added a new set of ray contribution from the central star to the calculations of population inversion.
- ❖ Added user control over the size and intensity (in terms of saturation intensity) of the star.
- ❖ Used the dynamical models called CODEX<sup>[6]</sup> for 3D velocity fields.
- ❖ Better intrinsic depth scaling and parallelisation for cheaper job runs.

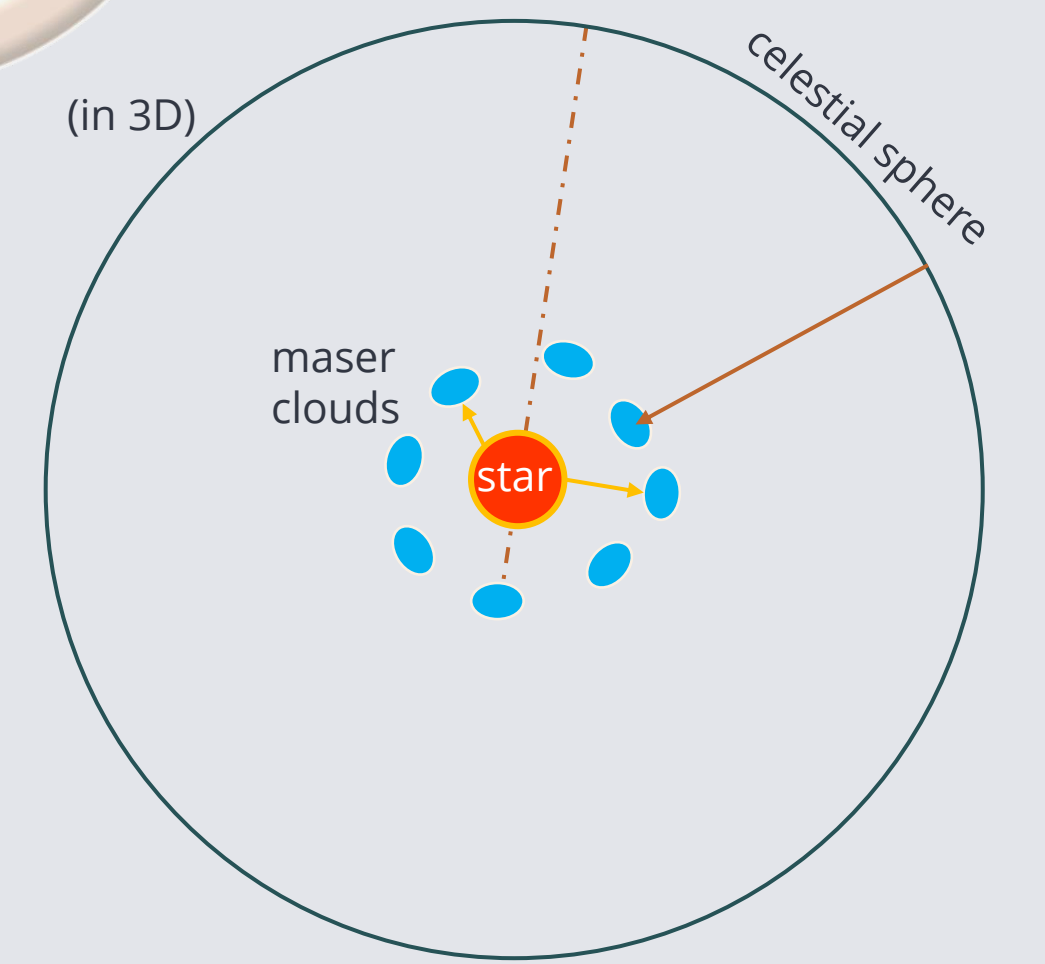


Figure 2. Schematic of how *maser3D* evaluates  $\Delta$  in a model of maser clouds around an AGB star. Solid arrows represent rays that are traced while the dashed line exemplifies a discarded ray, as it impinges on the (opaque) star.

## Results

### Flattened cloud model

- ❖ Shock-flattened clouds distributed in a shell around the star 1000 times brighter than the background

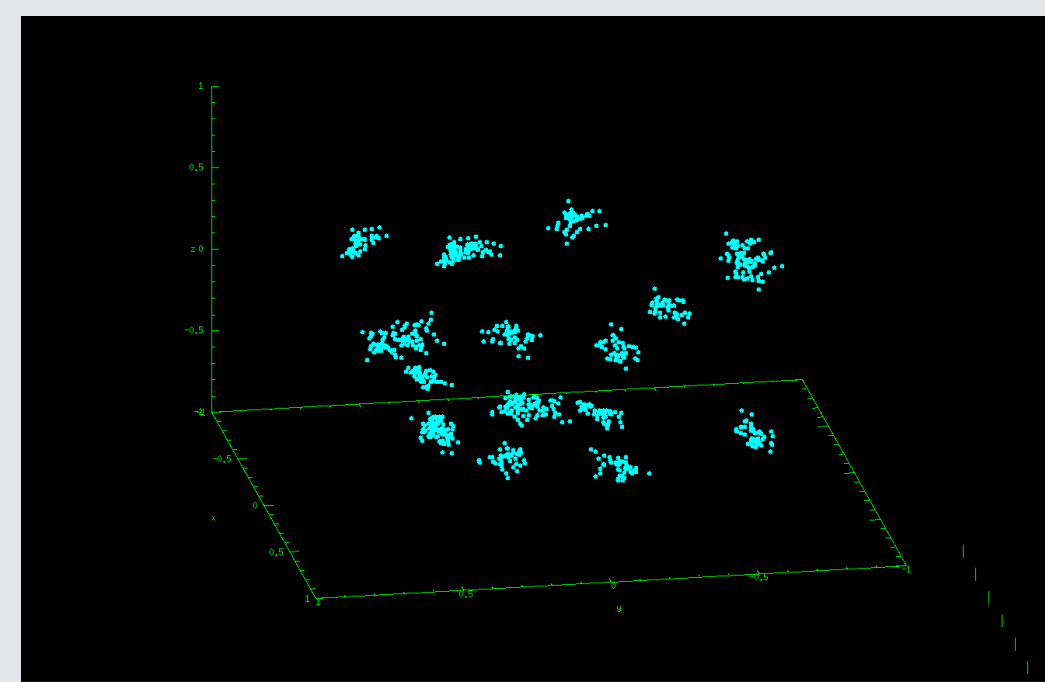


Figure 3. Plot of the flattened cloud domain. Note that they are elongated in the direction parallel to the 'shock front'.

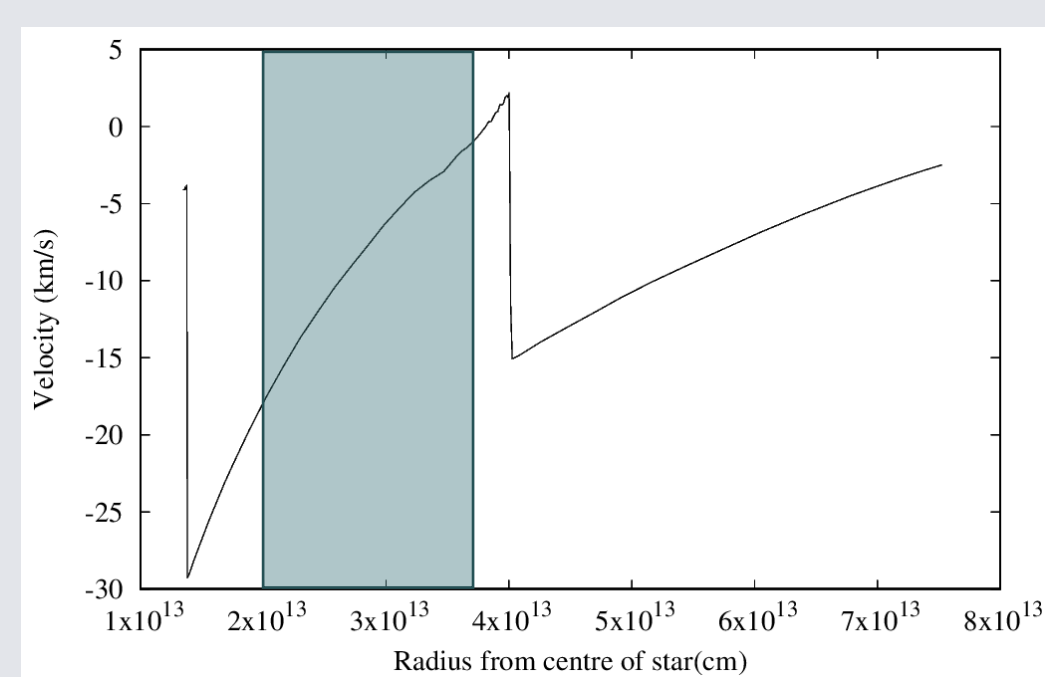


Figure 4. Plot of velocity as a function of radius from the CODEX series - 288320. The shaded area represents the range of radius in which the domain is situated.

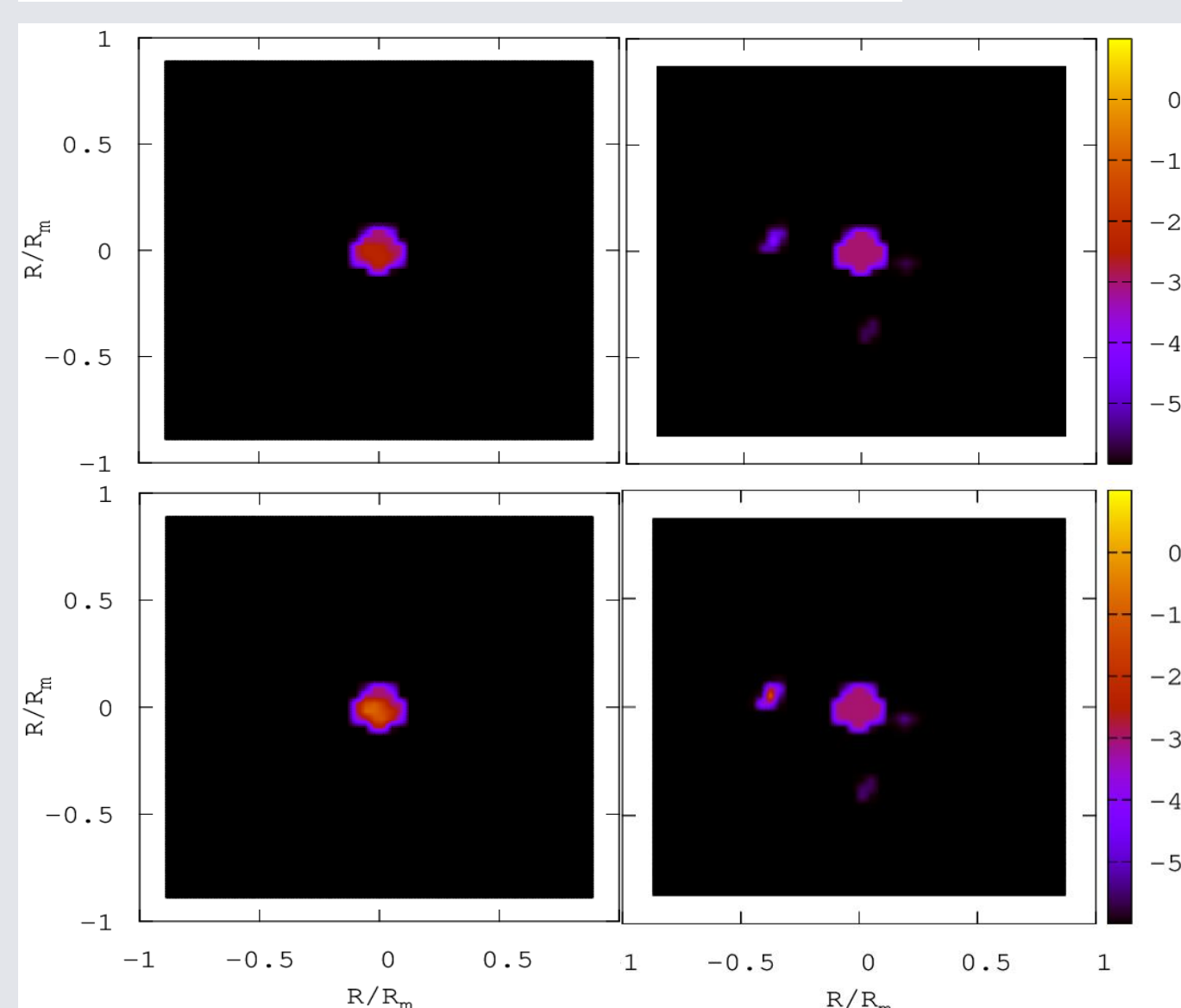
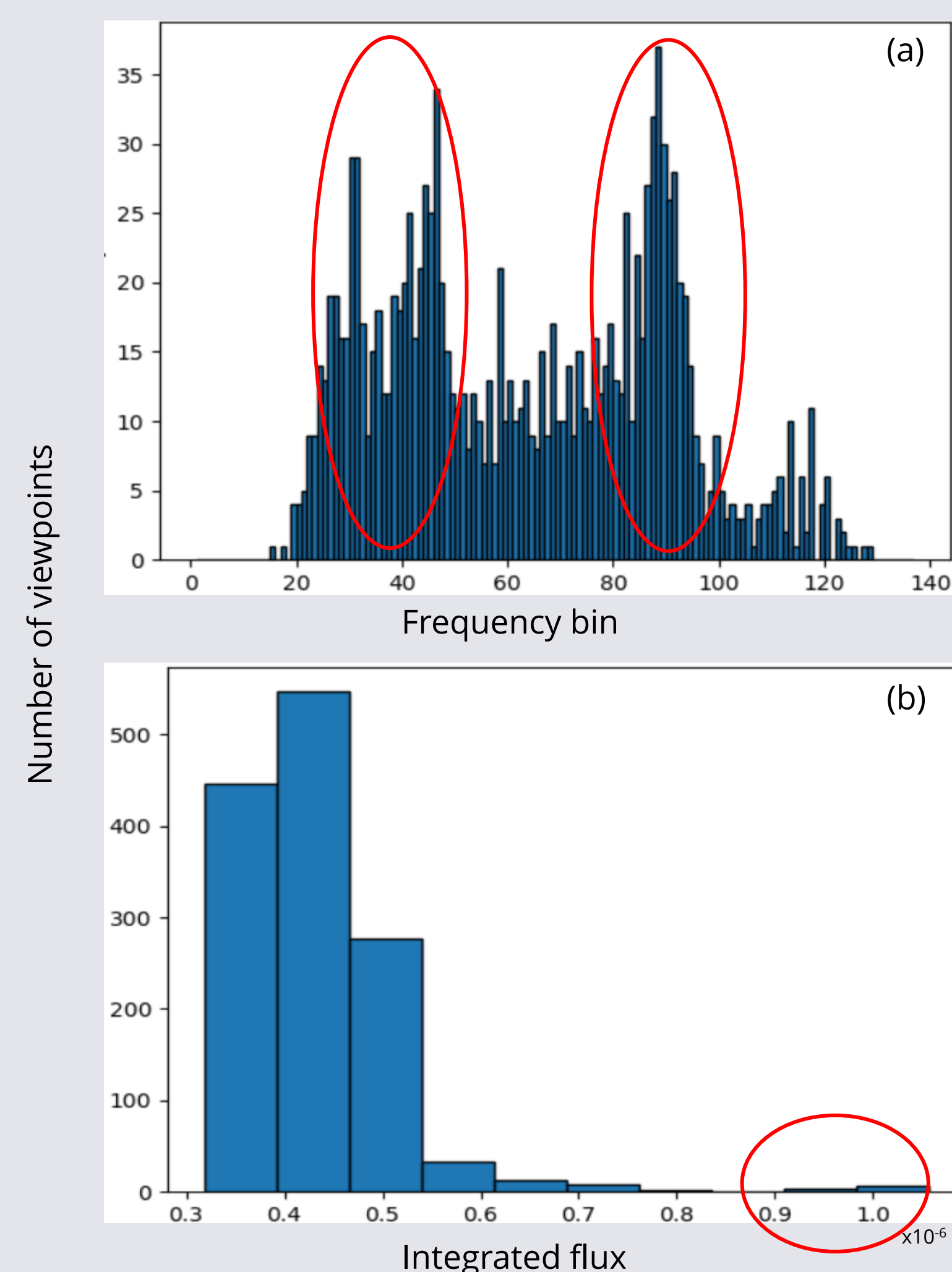


Figure 5. Simulated VLBI images showing how maser brightness and spot sizes change based on levels of saturation and viewing angles. The left panels are an example when there is a cloud in front of the star while those on the right show a viewpoint where clouds are in the shocked region around the star. The x and y axes are in normalised model size and the colour bar represents the log of specific intensity in terms of saturation intensity.

### Looking at the maser from 2,000 viewpoints

- ❖ If we considered a bigger picture, for a given maser in a CSE, what would be the most likely characteristics of the observations made?
- ❖ Random observer's positions defined by polar and azimuthal angles (with respect to the model axes); flux evaluated at the same distance of 1,000 model sizes.

Figure 6. Histograms showing (a) how the largest flux density is distributed in frequency bins and (b) the distribution of 'observed' integrated flux. The red circles highlight the most interesting features of these two plots (see discussion below)



### Modelling masers in $\pi^1$ Gru

Instead of a group of clouds, we produced our  $\pi^1$  Gru domain based on a smoothed particle hydrodynamics (SPH) model of the source.

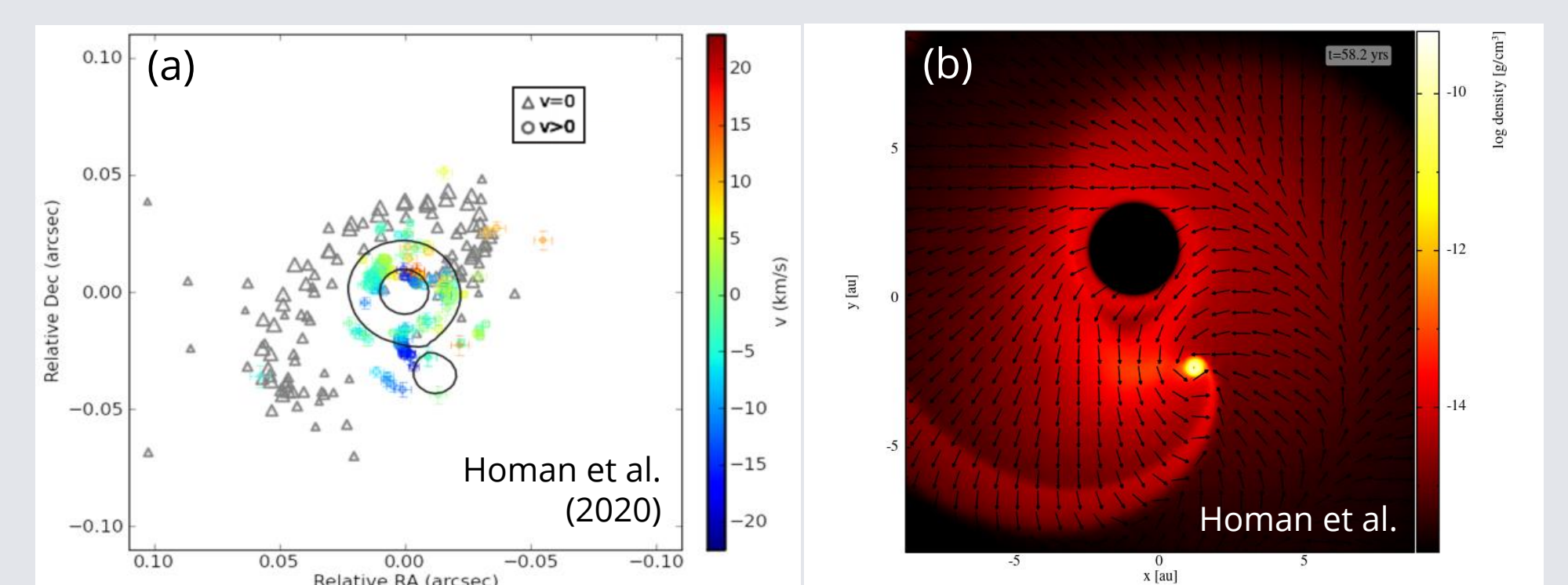


Figure 7. (a) Fitted vibrationally excited (in colour) and ground-state (grey) SiO maser component map from ALMA observations of  $\pi^1$  Gru<sup>1</sup>; (b) SPH simulation based on the observations in (a), courtesy of Homan et al.; and (c) the domain created for *maser3D*, each point representing a node which contains the density and velocity information from the SPH model.

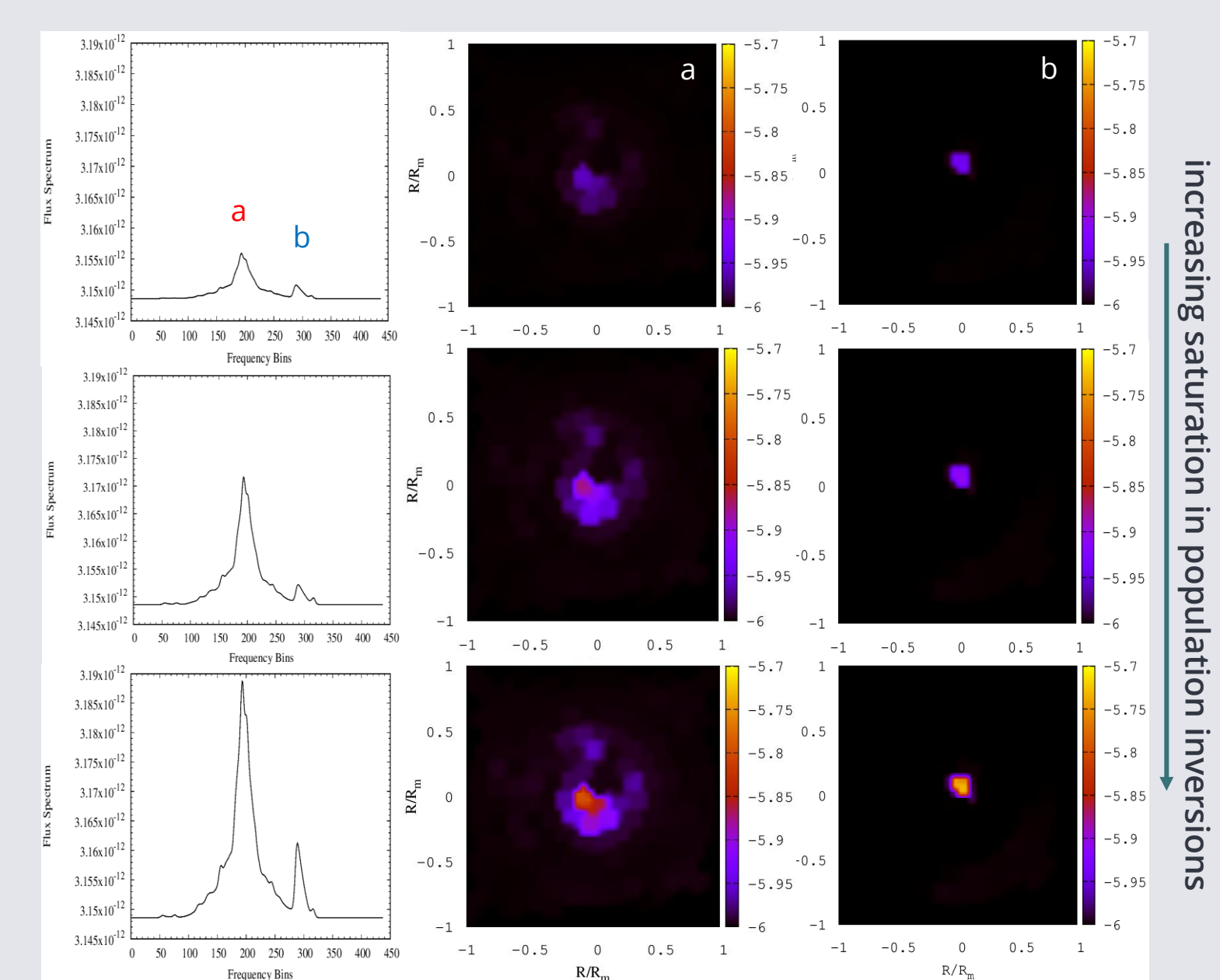


Figure 8. First results of the  $\pi^1$  Gru model. Note however that no contribution from the star has yet been considered in this case.

## Discussion

For the flattened cloud model, it can be deduced from Fig. 5 that different viewpoints result in different positions of bright maser spots, and these perhaps are dominated by different pumping mechanisms:

- ❖ Clouds in front of the star = *radiative* pumping
- ❖ Clouds in the shocked region around the star = *collisional* pumping

Based on the study of viewpoint statistics, it is apparent that, for a given maser originating in the CSE of an evolved star, we likely see the maser to be Doppler-shifted (Fig. 6a) and its flux is unremarkable unless the observer is looking at the source in the direction optimal for maximum maser amplification (Fig. 6b).

The simulated spectra (with flux density in model units) and VLBI images of the  $\pi^1$  Gru model (Fig. 8) are consistent with a typical maser flare observation. And as the maser becomes more saturated, especially near and around the companion, a rise in maser intensity can be seen as per the flattened cloud model.

## Discussion (cont.)

However, the problem with the current set of results is potentially incorrect depth scaling during the ray tracing procedure as the modelled maser brightness is suspiciously low for the levels of saturation being investigated.

The next step for the  $\pi^1$  Gru model is to place a star at the centre such that we have an extra source of radiation akin to the flattened cloud model. Input parameters e.g. the stellar radius in model size, the stellar intensity, etc., can be taken/estimated from available observational data.

## References

- [1] Goldreich, P., & Keeley, D. A., 1972, *Apl*, 174, 517.
- [2] Emmering, R. T., & Watson, W. D., 1994, *Apl*, 424, 991-1004.
- [3] Gray M., Mason L., Etoka S., 2018, *MNRAS*, 477, 2628.
- [4] Gray M., Baggott L., Westlake J., Etoka S., 2019, *MNRAS*, 486, 4216.
- [5] Gray M., Etoka S., Travis A., Pimpanuwat B., 2020, *MNRAS*, 493, 2472.
- [6] Ireland M. J., Scholz M., Wood P. R., 2011, *MNRAS*, 418, 114.
- [7] Homan et al., 2020, *A&A*, 644, A61.